Observation of inverted hysteresis loop and thermomagnetic irreversibility in the antiferromagnetic Mn$_5$Si$_3$ alloy

S. C. Das,[1] K. Mandal,[1] P. Dutta,[2] S. Pramanick,[1] and S. Chatterjee[1,*]

[1]*UGC-DAE Consortium for Scientific Research, Kolkata Centre, Sector III, LB-8, Salt Lake, Kolkata 700 106, India*
[2]*School of Physical Sciences, Indian Association for the Cultivation of Science,*
2 A & B Raja S. C. Mullick Road, Jadavpur, Kolkata 700 032, India

Mn$_5$Si$_3$ crystallizes in hexagonal D8$_8$ type structure (space group $P6_3/mcm$) with two distinct crystallographic sites for Mn atoms. It undergoes two first-order phase transitions during cooling from paramagnetic to collinear antiferromagnetic phase around 100 K and subsequently to noncollinear antiferromagnetic phase around 66 K. Detailed investigation by dc magnetic measurements probe the presence of inverted hysteresis loop below 66 K. In addition, thermomagnetic and field-induced arrest are the two key features of this alloy. Such arrest of high temperature phase plays the pivotal role toward the observation of inverted hysteresis loop behavior. The robustness of the arrested states was checked by magnetic relaxation measurements.

I. INTRODUCTION

Recently, metal silicides have attracted renewed attention due to their potential application in the field of microelectronics [1,2]. Apart from their interesting electronic properties, these materials also show diverse magnetic and magnetofunctional behaviors [3–5]. Among others, the Mn based silicide of nominal composition Mn$_5$Si$_3$ is under active scientific investigations due to its fascinating structural, magnetic, and magnetofunctional behaviors [6–13]. Mn$_5$Si$_3$ crystallizes in hexagonal D8$_8$ type structure (space group $P6_3/mcm$) with two distinct crystallographic sites for Mn atoms, namely, 4(d) (termed as Mn1) and 6(g) (termed as Mn2) [6,7]. This alloy is found to be paramagnetic (PM) in nature at room temperature (300 K). On cooling, at first it undergoes transition from PM to collinear antiferromagnetic (AFM2) phase at 100 K and then to a noncollinear antiferromagnetic (AFM1) phase at 66 K [6,7]. The PM to AFM2 transition is also associated with a change in magnetic structure and the system becomes orthorhombic with space group $Ccmm$. The orthorhombic cell parameters can be represented by the hexagonal cell parameters as $a_o \approx a_h$, $b_o \approx \sqrt{3}a_h$, and $c_o \approx c_h$ [8]. In this phase, the Mn2 site divides into two independent sites, namely, Mn21 and Mn22. Neutron diffraction study confirms the absence of ordered moments in Mn1 and Mn21 atoms, whereas Mn22 atoms ordered antiferromagnetically along the crystallographic b axis in collinear fashion [8]. On the other hand, AFM1 ordering results in an additional structural distortion and the symmetry of magnetic structure becomes monoclinic with the noncentrosymmetric $Cc2m$ space group. During this transition, the Mn22 site further splits into two inequivalent sites Mn23 and Mn24 [8]. In this AFM1 state below 66 K, Mn1 (with two equivalent sites Mn11 and Mn12), Mn23, and Mn24 carry moments with different magnitude [8].

Atoms in Mn21 sites remain momentless. Neutron diffraction studies confirm the highly noncollinear arrangement of Mn moments in the AFM1 state and the overall moment of the alloy is in general direction. Sürgers *et al.* recently reported the presence of another intermediate magnetic configuration, AFM1′, through which the AFM1 state transforms to an AFM2 state in the presence of an applied magnetic field (H) [12]. In the AFM1′ state, the moment of the Mn1 site (Mn11 and Mn12) vanishes again, though the highly noncollinear arrangement of Mn23 and Mn24 remains unchanged [12]. In addition to such unusual magnetic properties, Mn$_5$Si$_3$ also shows different functional properties, such as large inverse magnetocaloric effect, anomalous Hall effect, etc. [9,12,14]. A recent study by Biniskos *et al.* indicates that spin fluctuation plays the pivotal role toward the observation of such large inverse magnetocaloric effect [13].

The presence of first-order phase transition (FOPT) often triggers thermomagnetic irreversibility in the system. A magnetically arrested state is the key observation of such thermomagnetic irreversibility. This effect is commonly observed in Heusler based shape memory alloys and phase separated manganites [15–23]. The presence of FOPT in undoped Mn$_5$Si$_3$ alloy may induce thermomagnetic irreversibility in the system. Though the Mn$_5$Si$_3$ alloy is under active research, investigation on such thermomagnetic irreversibility is still lacking. In the present work, we have thoroughly investigated the Mn$_5$Si$_3$ alloy through detailed dc magnetic measurements and observed intriguing history dependence of magnetic moments in the low temperature region with temperature (T) and magnetic field (H). In addition, we also observe a clear signature of inverted hysteresis loop, which probably is an outcome of thermomagnetic irreversibility.

II. EXPERIMENTAL DETAILS

The binary intermetallic alloy of nominal composition Mn$_5$Si$_3$ was prepared by arc melting the required amount of
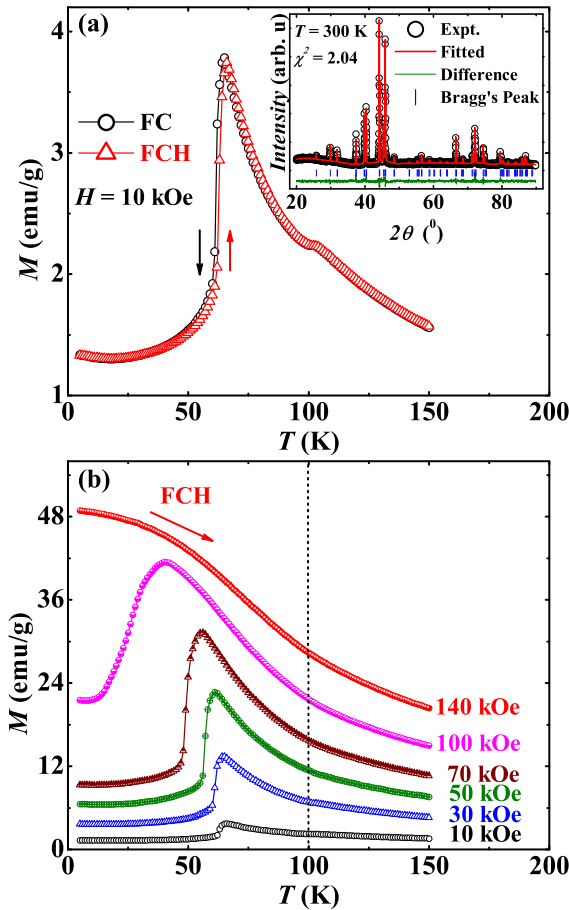
*souvik@alpha.iuc.res.in

FIG. 1. Inset of (a) depicts room temperature x-ray powder diffraction data along with Rietveld fitted curve, difference pattern, and Bragg's peak position. Temperature (T) variation of dc magnetization (M) in field cooling (FC) and field-cooled heating (FCH) protocols in the presence of 10 kOe of external magnetic field (H) is plotted in the main panel of (a). (b) shows $M(T)$ data in FCH protocol at different constant H.

high pure ($\geqslant 99.9\%$) Mn and Si in an inert argon atmosphere. The alloy was remelted four times for homogeneity. The ingot was then sealed in an evacuated quartz tube and annealed at 900 °C for 168 h followed by ice-water quenching. The alloy was characterized by room temperature x-ray powder diffraction measurements using a Bruker AXS diffractometer (D8-Advance) fitted with Cu $K\alpha$ radiation [see inset of Fig. 1(a)]. Rietveld analysis of the recorded data using the FULLPROF software package [24] indicates a pure hexagonal D8$_8$ type structure (space group $P6_3/mcm$) at room temperature with lattice parameters $a = 6.914$ Å and $b = 4.816$ Å. The observed lattice parameters match well with the previously reported data [10]. No signature of impurity phases have been observed in the recorded diffraction pattern. dc magnetic measurements were performed by using a cryogen-free 150 kOe system from Cryogenic Ltd., UK. During measurements, the sample space was filled with helium exchange gas for better temperature stability. About 15 mK fluctuation in temperature has been observed during isothermal measurements. To ensure the true zero-field-cooled (ZFC) condition, we switched off the helium compressor connected to our superconducting

magnet and warmed the magnet until the magnet temperature crosses its superconducting transition temperature. This procedure makes the magnetic field zero by removing the trapped field, which is very common for a superconducting magnet. This method was followed for all zero-field-cooled measurements.

III. EXPERIMENTAL RESULTS

T variation of dc magnetization (M), recorded in the presence of 10 kOe of external H in field cooling (FC) and field-cooled heating (FCH) protocols are depicted in the main panel of Fig. 1(a). On cooling from 150 K, M is found to increase monotonically until 100 K. At 100 K, it shows a change in slope, signifying PM to AFM2 transition. Further decrease in sample temperature results in an increase in M value and at 66 K it shows a peaklike feature. Below 66 K, M is found to decrease sharply and eventually saturates below 25 K. The anomaly at 66 K indicates the AFM2 to AFM1 transition in the alloy. Two magnetic transitions observed in the presently studied alloy matches well with the previously reported data [14]. We repeated the $M(T)$ measurements in the FCH protocol at different applied H [see Fig. 1(b)]. Interestingly, the AFM2 to AFM1 transition temperature is found to be shifted toward lower T with increasing H, while the PM to AFM2 transition remains unaltered. No traces of collinear to noncollinear AFM transition has been observed for 140 kOe data. Such shift in AFM2 to AFM1 transition temperature is due to the presence of field-induced AFM1 to AFM2 transition via the AFM1′ state [12]. This indicates that application of H prefers the AFM2 state over the AFM1 state. Such field-induced transition has already been confirmed by dc magnetic, neutron diffraction, and Hall measurements [8,9,12]. We also recorded isothermal M as a function of H at different constant T in ZFC condition [see Figs. 2(a) and 2(b)]. A small change in slope in $M(H)$ isotherms have been observed in the low field region below 66 K indicating AFM1 to AFM1′ transition. This slope change field is found to be 70 kOe at 5 K. In addition to that, the $M(H)$ isotherms below 66 K show a sharp change in M values. Such sharp change in M value is due to the AFM1′ to AFM2 transition. Both the transition fields are found to be shifted toward the lower value with increasing sample temperature [see Fig. 2(b)]. The critical fields of transitions observed for the present alloy also matches with the previously reported data [12,25].

Apart from this field-induced AFM1-AFM1′-AFM2 transition visible in the $M(H)$ isotherms, another unexplored feature is also associated with it. Now, let us concentrate on such feature. A closer look at the hysteresis region of the 5 K $M(H)$ isotherm reveals that it is inverted in nature, i.e., the loop has positive coercive field and negative remanence [see the main panel of Fig. 3(a); virgin line is not shown here for clear visualization]. Usually, remanence is found to be positive after reducing the strength of applied H to zero from saturation field as M relaxes to the easy axes with M oriented toward the same direction of H. On the other hand, for the inverse case, though the remanent state M lies at the easy axes, the majority of M oriented toward the opposite direction of applied H. Such anomalous behavior of $M(H)$ isotherm was first observed in amorphous Gd-Co
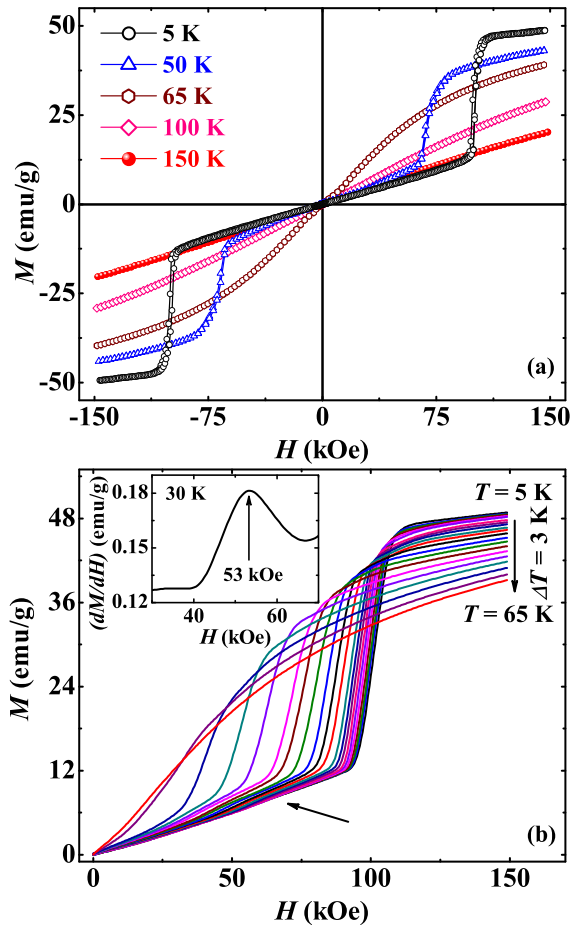
FIG. 2. Isothermal variation of dc magnetization (M) as a function of magnetic field (H) at different constant temperature (T) recorded between ±150 kOe in ZFC condition are plotted in (a). Main panel of (b) shows first the H increasing line of $M(H)$ curves recorded at 3 K intervals between 5 and 65 K. Inset of (b) depicts $\frac{dM}{dH}$ vs H curve at 30 K for a restricted region. The critical field for AFM1-AFM1$'$ transition is indicated by an arrow.

films [26]. Apart from this, there are several examples of the observation of an inverted hysteresis loop (IHL) in exchange coupled multilayers, hard/soft multilayers, and single domain particles with competing anisotropies [27–39]. Recently, IHL has also been observed in a bulk ferrimagnet of composition Er_2CoMnO_6 [40]. However, this novel feature is quite uncommon in polycrystalline alloys having AFM ground state. It is clear from the 5 K $M(H)$ data that the field decreasing and field increasing lines cross each other around $H_{cross} = \pm23$ kOe [marked by an arrow in Fig. 3(a)]. To check whether the field-induced transitions have any role on the observed IHL, we recorded $M(H)$ isotherms at 5 K in ZFC condition with different maximum/upper bound field of measurements, namely, ±100 kOe (between AFM1$'$-AFM2 transition field), ±70 kOe (around the AFM1-AFM1$'$ transition field), and ±50 kOe (well below the AFM1-AFM1$'$ transition field). Such $M(H)$ isotherms are presented in Figs. 3(b), 3(c) and 3(d), respectively. It is interesting to note that the inversion in $M(H)$ isotherms depend strongly on the maximum applied H and the inversion is only visible for applied $H > 70$ kOe

(above AFM1-AFM1$'$ transition field). We also checked the T dependence of H_{cross} by recording $M(H)$ isotherms between ±150 kOe at different constant T up to 70 K. The value of H_{cross} shows a sluggish drop up to 30 K followed by a rapid decrease with increasing T and eventually the inversion vanishes above 66 K, which is basically the AFM1 to AFM2 transition point. Variation of H_{cross} as a function of T is plotted in the upper inset of Fig. 3(a). Similar crossing has also been observed in the Hall resistivity data along the "c" axis for Mn_5Si_3 single crystals [12]. Exchange bias effect associated with the grain boundaries for polycrystalline alloys may give rise to such IHL behavior. To check such possibility, we performed exchange bias measurements for the present alloy at 5 K. During these measurements we cooled the sample in the presence of different applied H. We have not observed any shift in the center of $M(H)$ isotherms [see lower inset of Fig. 3(a) for zero-field-cooled and 10 kOe field-cooled data]. All the $M(H)$ curves are found to be perfectly symmetric. In addition, we repeated such field-cooled $M(H)$ measurements at higher temperature also (not shown here). We have not observed any signature of exchange bias effect at any temperature below 66 K. This indicates that the observed IHL has some different origin.

To probe the true reason behind the observation of IHL in the presently studied alloy, we recorded several $M(T)$ data with different protocols. Firstly, we cooled the sample in the presence of different applied field (H_{cool}) from 150 K (well above the AFM2 to PM transition temperature) and recorded M as a function of T during heating in the presence of 0.1 kOe of external H [see Fig. 4(a)]. It is clear from Fig. 4(a) that the dc magnetic moment below AFM2-AFM1 transition region depends strongly on the H_{cool} even though they are measured in the presence of same heating field (H_{warm}). The magnitude of the moment of AFM1 phase increases with cooling field up to 5 kOe. Further increase in H_{cool} results in a decrease in the moment value and eventually it becomes negative for 40 kOe of applied H_{cool}. Such strong H_{cool} dependence of $M(T)$ data is not uncommon among the materials having first-order phase transition and commonly known as field-induced arrested phenomenon [15,41–45]. Magnetothermal arrest of the high temperature phase is playing the key role behind such unusual $M(T)$ behavior in the low-T region. As per the phase diagram obtained by Sürgers et $al.$, the presently studied alloy transforms from AFM2 to AFM1 phase via the AFM1$'$ state when cooled in the presence of external H. It is pertinent to investigate the true character of the magnetothermally arrested state. In other words, our aim is to identify between the two high-T phases (AFM2 and AFM1$'$), which one is getting arrested during field cooling. It is also important to know whether any critical temperature is present below which the high-T phase is getting arrested. To shed more light, we recorded $M(T)$ data in the presence of 0.1 kOe of external H after cooling the sample from different T ($T_{mag} = 150, 80, 40,$ and 30 K) in 50 kOe of applied H [see Fig. 4(b)]. During these measurements, the sample was first cooled in zero field from 180 K to the respective temperatures of field application T_{mag}. This investigation indicates that the magnitude of M is negative and minimum for $T_{mag} = 150$ K. The magnitude of M remains almost constant at 5 K with decreasing value of T_{mag} down to 80 K. Further decrease in T_{mag} results in a large
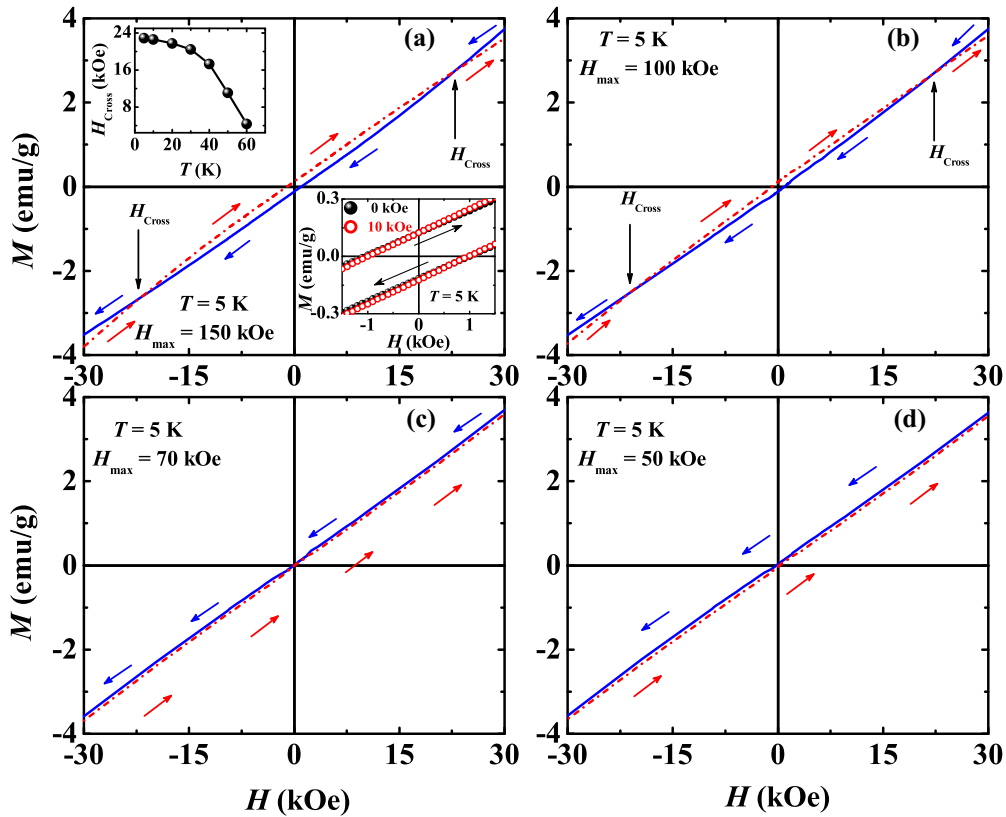
FIG. 3. (a) A restricted region of the 5 K $M(H)$ isotherm recorded in ZFC condition between ± 150 kOe is plotted in the main panel. Crossing of increasing and decreasing field line curves are indicated by arrows. Upper inset shows the variation of crossing field H_{cross} as a function of temperature. Lower inset depicts the restricted view of zero field cooled and 10 kOe field cooled isothermal $M(H)$ data at 5 K. Restricted region of isothermal variation of dc magnetization (M) as a function of magnetic field (H) at 5 K recorded between ± 100 kOe, ± 70 kOe and ± 50 kOe in ZFC condition are plotted in (b), (c) and (d) respectively.

increase in M and eventually it becomes positive for $T_{mag} = 30$ K. We further checked the $M(T)$ behavior by cooling the sample from $T_{mag} = 30$ K in the presence of 60 kOe of applied H. Interestingly, the magnitude of M becomes negative again for 60 kOe cooling field even for $T_{mag} = 30$ K (well below the AFM2 to AFM1 transition point) as plotted in Fig. 4(c). This observation indicates that H_{cool} rather than T_{mag} plays the key role behind the observed magnetothermal arrest. Now, if one closely observes the critical field of AFM1 to AFM1′ transition from $M(H)$ isotherms, it may be noted that it is around 53 kOe at 30 K, which is further clear from the $\frac{dM}{dH}$ vs H plot [see inset of Fig. 2(b)]. So, the applied H should be greater than the critical H of AFM1 to AFM1′ transition at T_{mag} to observe a negative moment at 5 K. It indicates that part of the AFM1′ state rather than the AFM2 state is getting arrested during field cooling. In addition, from $M(T)$ data one can also conclude that the arrested AFM1′ state remains arrested even if the applied H is reduced to 0.1 kOe. Next, we have checked whether the situation is similar for isothermal field application also by recording $M(T)$ data in different protocols [see Fig. 4(d)]. Here we have cooled the sample in zero field from 150 to 5 K and applied different fields with magnitudes 50, 70, 100, and 150 kOe. In each occasion, we have waited for 5 min and reduced the applied H to 0.1 kOe and recorded M as a function of T during heating. In

this protocol also we have observed large mismatch in the magnitude of M at the low-T region. In addition, we also observed a negative value of M for 100 and 150 kOe field application. On application of external H at 5 K in ZFC condition, the studied alloy transforms from an AFM1 state to an AFM1′ or AFM2 state (via AFM1′) depending on the field magnitude at the low-T region [12]. But on removal of H, the alloy is unable to regain its ZFC state even in presence of 0.1 kOe of external H. Part of the AFM1′ state remains arrested. This observation further supports the IHL behavior. The field-induced isothermal arrest plays the key role behind the observed negative moment and inverted loop.

We also checked the rigidness of the observed arrested state by relaxation measurements with two different protocols, name, (i) ZFC mode and (ii) FC mode (see Fig. 5). In the ZFC mode, we first cooled the alloy in zero-field condition to 5 K from 150 K and applied 100 kOe of external H. After waiting for 5 min, we reduced the applied H to zero and recorded dc M as a function of time (t). On the other hand, for FC protocol, we cooled the studied alloy in the presence of 100 kOe of external H from 150 K to 5 K. After reaching 5 K, we reduced the applied H to zero and recorded dc M as a function of t. The reason behind recording the relaxation data in ZFC and FC protocols is to check the rigidity of isothermal and magnetothermal arrested states, respectively. For both the
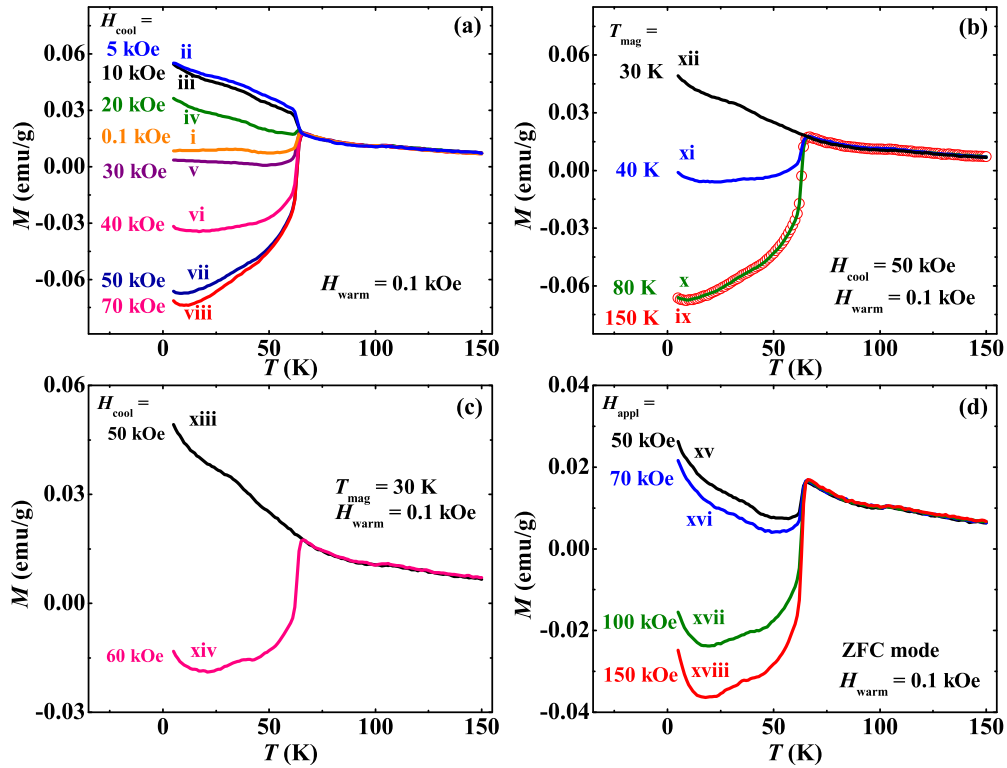
FIG. 4. Magnetization (M) recorded as a function of temperature (T) while heating in 0.1 kOe of external magnetic field (H) (a) after being cooled in H_{cool} = (i) 0.1, (ii) 5, (iii) 10, (iv) 20, (v) 30, (vi) 40, (vii) 50, and (viii) 70 kOe; (b) after being field cooled in 50 kOe of H from T_{mag} (ix) 150, (x) 80, (xi) 40, and (xii) 30 K; (c) after being field cooled from 30 K in H_{cool} = (xiii) 50 and (xiv) 60 kOe; and (d) after zero-field cooling and field cycling at 5 K with maximum H value of H_{appl} = (xv) 50, (xvi) 70, (xvii) 100, and (xviii) 150 kOe.

protocols, dc M data were recorded for 3 h each. Due to the presence of a mixture of AFM1 and AFM1′ phases in both ZFC and FC protocols, magnitudes of dc M were negative (due to the absence of the Mn1 site moment in the AFM1′ phase). The observed change in M values is toward the more

negative direction, and though the change is very small, this indicates the stable nature of both types of arrested states.

IV. DISCUSSIONS AND CONCLUSION

We performed a systematic investigation on the magnetic properties of a Mn-based binary alloy having nominal composition Mn_5Si_3. An inverted hysteresis loop and thermomagnetic irreversibility due to arrested AFM1′ (both thermomagnetic and isothermal arrest) are the two key observations of the studied alloy. The inversion behavior of the $M(H)$ isotherm strongly depends on the magnitude of the maximum applied H and it is only visible if the applied maximum H is greater than the critical field of AFM1-AFM1′ transition, which is 70 kOe at 5 K. It indicates that the AFM1′ phase rather than the AFM2 phase plays a pivotal role toward the observation of IHL in the present alloy [as the loop inversion is visible for $M(H)$ isotherm with 100 kOe of maximum applied H, which is just below the critical field for AFM1′-AFM2 transition]. To shed more light on this IHL behavior, several isofield $M(T)$ data were recorded with different protocols. The value of dc M in the low-T region is found to be very different for each protocol (as shown in Fig. 4). Interestingly, for some protocols, the value of dc M becomes negative. The observed behavior is due to the presence of thermomagnetic and field-induced arrest of the AFM1′ state. Previous studies indicate that at 4.2 K with noncollinear AFM structure, the moments present at the Mn1 (Mn11 and Mn12), Mn23, and
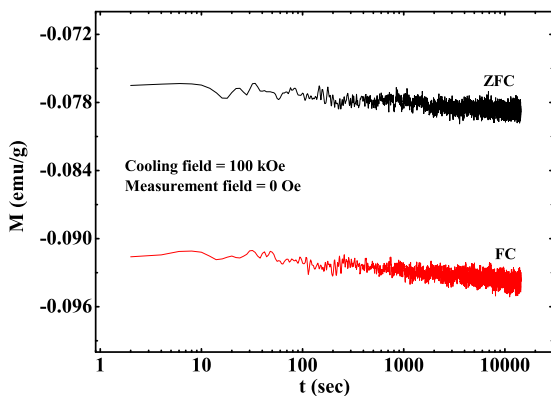

FIG. 5. dc magnetization (M) is plotted as a function of time (t) at 5 K in zero-field-cooled (ZFC) and field-cooled (FC) protocols. After reaching 5 K in ZFC protocol, 100 kOe field was applied and waited for 5 min, and time evolution of M was measured immediately after removing the field. For FC protocol, 100 kOe field was applied during cooling and measurement was carried out immediately after removing the field at 5 K.
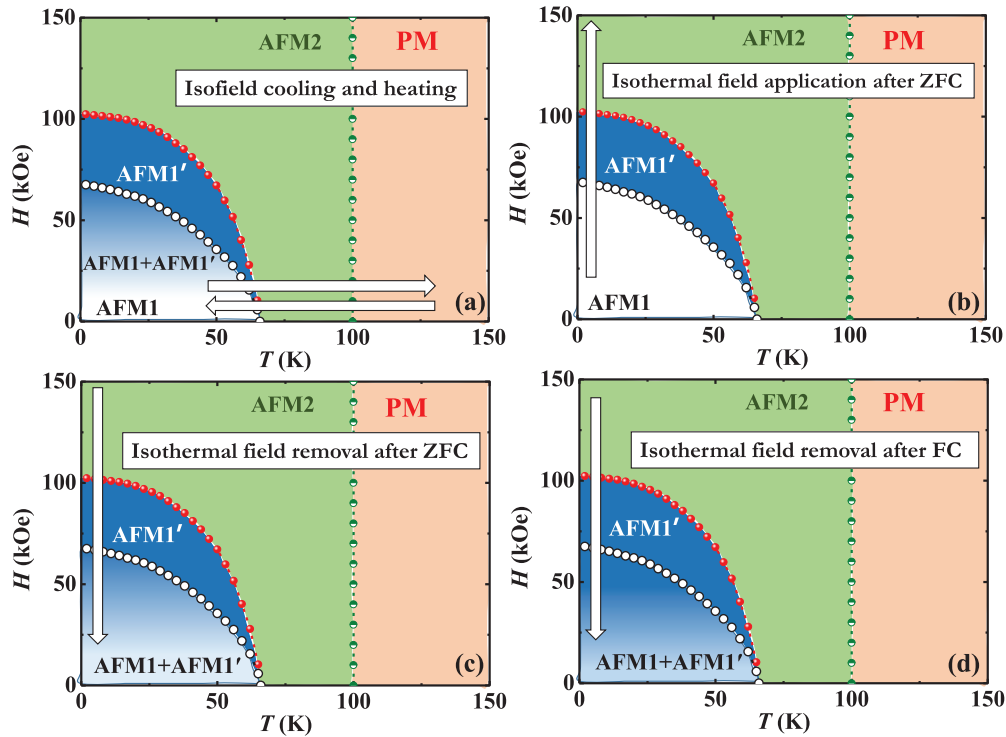
FIG. 6. Field-temperature (H-T) phase diagrams for (a) isofield cooling and heating, (b) isothermal field application after zero-field cooling (ZFC), (c) isothermal field removal after 150 kOe of field application in ZFC, and (d) isothermal field removal after FC in 150 kOe. Color gradient indicates the phase coexistence.

Mn24 sites are $1.20\mu_B$, $2.30\mu_B$, and $1.85\mu_B$, respectively [8]. In ZFC condition, Mn1, Mn23, and Mn24 sites carry moments and orders in noncollinear AFM fashion. In this situation, these moments balance each other. On the other hand, for the field-induced or thermomagnetically arrested state at 5 K, the studied alloy has a mixture of the AFM1 and the AFM1$'$ state. A recent report by Sürgers et al. indicates that in the AFM1$'$ state, the Mn1 (Mn11 and Mn12) site moment vanishes, whereas the Mn23 and Mn24 site moments remain unchanged with noncollinear arrangement. Absence of this Mn1 site moment affects the balance of three Mn site moments and results in a negative moment in the low-H region. Notably, the thermomagnetically arrested AFM1$'$ state starts to appear for the applied cooling field greater than 5 kOe (as the moment value at the low-T region decreases after an initial increase above 5 kOe of applied H), but the negative moment is only observed for $H_{cool} > 30$ kOe. This is due to the fact that the increase in cooling field results in an increase in the arrested AFM1$'$ phase fraction and when the arrested phase is sufficiently large (with a large number of Mn1 sites having zero moment), the negative moment appears. For the isothermal case, the negative moment is only observed above $H = 70$ kOe. This is because of the fact that the AFM1$'$ state appears only above 70 kOe at 5 K. This scenario is pictorially represented in Fig. 6. Our observation indicates that the H-T phase diagram of the present sample depends strongly on the history of field application. Based on our new observations in the studied material, we have modified the H-T phase diagram proposed by Sürgers et al. [12] In the proposed phase diagram we have used four colors to specify the four phases of the alloy, namely, orange for PM phase,

green for AFM2 phase, blue for AFM1$'$ phase, and white for AFM1 phase. The blue color gradient has been used for indicating the phase coexistence. On the modified H-T phase diagram, AFM2-AFM1$'$ and AFM1$'$-AFM1 transition fields at different temperatures were determined by differentiating isothermal $M(H)$ data recorded at different constant T, while PM-AFM2 transition temperatures at different applied H were determined from isofield $M(T)$ data. Figure 6(a) depicts the isofield heating and cooling case only. On the other hand, the isothermal cases are explained by Figs. 6(b)–6(d). The phase diagram for isothermal field application ($H = 150$ kOe) after ZFC is identical to the H-T phase diagram presented by Sürgers et al. [12]. But removing 150 kOe of applied H after ZFC and FC gives different phase mixture, represented by different shades of blue. In the FC case, the presence of more AFM1$'$ phase after removal of external H is further clear from the more negative value of M in the FC relaxation data (see Fig. 5). Also the relaxation behaviors at 5 K in ZFC and FC conditions indicate a very stable nature of both the isothermally and magnetothermally arrested AFM1$'$ state at 5 K. This is unlike the nature of arrested states that have been observed in Heusler-based shape memory alloys and phase separated manganites [15–23].

In conclusion, our investigation reveals the presence of two new properties, namely, inverted hysteresis loop and thermomagnetic irreversibility, in the presently studied alloy. The arrested AFM1$'$ state is playing the key role behind such novel features. We have tried to modify the existing H-T phase diagram by incorporating the features observed in the present investigation. Here we report the observation of such interesting and unique properties in Mn$_5$Si$_3$ alloy.

ACKNOWLEDGMENTS

[1] F. Jonietz, S. Mühlbauer, C. Pfleiderer, A. Neubauer, W. Münzer, A. Bauer, T. Adams, R. Georgii, P. Böni, R. A. Duine, K. Everschor, M. Garst, and A. Rosch, Science **330**, 1648 (2010).

[2] X. Z. Yu, Y. Onose, N. Kanazawa, J. H. Park, J. H. Han, Y. Matsui, N. Nagaosa, and Y. Tokura, (London) **465**, 901 (2010).

[3] Y. Onose, N. Takeshita, C. Terakura, H. Takagi, and Y. Tokura, Phys. Rev. B **72**, 224431 (2005).

[4] S. M. Stishov, A. E. Petrova, S. Khasanov, G. K. Panova, A. A. Shikov, J. C. Lashley, D. Wu, and T. A. Lograsso, Phys. Rev. B **76**, 052405 (2007).

[5] A. Bauer, M. Garst, and C. Pfleiderer, Phys. Rev. Lett. **110**, 177207 (2013).

[6] G. H. Lander, P. J. Brown, and J. B. Forsyth, Proc. Phys. Soc. **91**, 332 (1967).

[7] A. Z. Menshikov, A. P. Vokhmyanin, and Y. A. Dorofeev, Phys. Status Solidi B **158**, 319 (1990).

[8] M. R. Silva, P. J. Brown, and J. B. Forsyth, J. Phys.: Condens. Matter **14**, 8707 (2002).

[9] M. Gottschilch, O. Gourdon, J. Persson, C. de la Cruz, V. Petricek, and T. Brueckel, J. Mater. Chem. **22**, 15275 (2012).

[10] P. J. Brown, J. B. Forsyth, V. Nunez, and F. Tasset, J. Phys.: Condens. Matter **4**, 10025 (1992).

[11] H. J. Al-Kanani and J. G. Booth, J. Magn. Magn. Mater. **140–144**, 1539 (1995).

[12] C. Sürgers, T. Wolf, P. Adelmann, W. Kittler, G. Fischer, and H. v. Löhneysen, Sci. Rep. **7**, 42982 (2017).

[13] N. Biniskos, K. Schmalzl, S. Raymond, S. Petit, P. Steffens, J. Persson, and T. Brückel, Phys. Rev. Lett. **120**, 257205 (2018).

[14] Songlin, Dagula, O. Tegus, E. Brück, J. C. P. Klaasse, F. R. de Boer, and K. H. J. Buschow, J. Alloys Compd. **334**, 249 (2002).

[15] S. Chatterjee, S. Giri, S. Majumdar, and S. K. De, Phys. Rev. B **77**, 224440 (2008).

[16] S. Chatterjee, S. Giri, and S. Majumdar, J. Phys.: Condens. Matter **24**, 366001 (2012).

[17] V. Siruguri, P. D. Babu, S. D. Kaushik, A. Biswas, S. K. Sarkar, M. Krishnan, and P. Chaddah, J. Phys.: Condens. Matter **25**, 496011 (2013).

[18] A. A. Wagh, P. S. A. Kumar, and S. Elizabeth, Mater. Res. Express **3**, 106102 (2016).

[19] D. J. Keavney, Y. Choi, M. V. Holt, V. Uhlir, D. Arena, E. E. Fullerton, P. J. Ryan, and J.-W. Kim, Sci. Rep. **8**, 1778 (2018).

[20] T. Kimura, Y. Tomioka, R. Kumai, Y. Okimoto, and Y. Tokura, Phys. Rev. Lett. **83**, 3940 (1999).

[21] V. K. Sharma, M. K. Chattopadhyay, and S. B. Roy, Phys. Rev. B **76**, 140401(R) (2007).

[22] A. K. Nayak, M. Nicklas, C. Shekhar, and C. Felser, J. Appl. Phys. **113**, 17E308 (2013).

[23] W. Ito, K. Ito, R. Y. Umetsu, and R. Kainuma, Appl. Phys. Lett. **92**, 021908 (2008).

[24] J. Rodriguez-Carvajal, Phys. B (Amsterdam, Neth.) **192**, 55 (1993).

[25] L. Vinokurova, V. Ivanov, E. Kulatov, and A. Vlasov, J. Magn. Magn. Mater. **90-91**, 121 (1990).

[26] S. Esho, Jpn. J. Appl. Phys., Suppl. **15**, 93 (1976).

[27] M. J. O'Shea and A.-L. Al-Sharif, J. Appl. Phys. **75**, 6673 (1994).

[28] A. Aharoni, J. Appl. Phys. **76**, 6977 (1994).

[29] K. Takanash, H. Kurokawa, and H. Fujimori, Appl. Phys. Lett. **63**, 1585 (1993).

[30] Y. Z. Wu, G. S. Dong, and X. F. Jin, Phys. Rev. B **64**, 214406 (2001).

[31] S. M. Valvidares, L. M. Álvarez-Prado, J. I. Martín, and J. M. Alameda, Phys. Rev. B **64**, 134423 (2001).

[32] S. Demirtas, M. R. Hossu, M. Arikan, A. R. Koymen, and M. B. Salamon, Phys. Rev. B **76**, 214430 (2007).

[33] M. Ziese, I. Vrejoiu, and D. Hesse, Appl. Phys. Lett. **97**, 052504 (2010).

[34] D. Y. Kim, C. G. Kim, C. O. Kim, S. S. Yoon, M. Naka, M. Tsunoda, and M. Takahashi, J. Magn. Magn. Mater. **304**, e356 (2006).

[35] S. I. Ohkoshi, T. Hozumi, and K. Hashimoto, Phys. Rev. B **64**, 132404 (2001).

[36] M. Cougo dos Santos, J. Geshev, J. E. Schmidt, S. R. Teixeira, and L. G. Pereira, Phys. Rev. B **61**, 1311 (2000).

[37] Y. J. Nam and S. H. Lim, Appl. Phys. Lett. **99**, 092503 (2011).

[38] J. Geshev, A. D. C. Viegas, and J. E. Schmidt, J. Appl. Phys. **84**, 1488 (1998).

[39] C. Song, B. Cui, H. Y. Yu, and F. Pan, J. Appl. Phys. **114**, 183906 (2013).

[40] A. Banerjee, J. Sannigrahi, S. Giri, and S. Majumdar, Phys. Rev. B **98**, 104414 (2018).

[41] S. Pramanick, S. Chattopadhyay, S. Giri, S. Majumdar, and S. Chatterjee, J. Appl. Phys. **116**, 083910 (2014).

[42] P. Dutta, D. Das, S. Chatterjee, and S. Majumdar, J. Alloys Compd. **590**, 313 (2014).

[43] P. Chaddah, K. Kumar, and A. Banerjee, Phys. Rev. B **77**, 100402(R) (2008).

[44] R. Rawat, K. Mukherjee, K. Kumar, A. Banerjee, and P. Chaddah, J. Phys.: Condens. Matter **19**, 256211 (2007).

[45] Y. Tokura, H. Kuwahara, Y. Moritomo, Y. Tomioka, and A. Asamitsu, Phys. Rev. Lett. **76**, 3184 (1996).